Thermal-Actuated Optoelectronic Memory Medium Based on Carbon Nanotube− and Nickel−Poly(dimethylsiloxane) Composites

Chunhua Hu,[†] Changhong Liu,*[,†] Yujuan Zhang,[‡] Luzhuo Chen,[†] and Shoushan Fan[†]

Department of Physics and Tsinghua−Foxconn Nanotechnology Research Center, Tsinghua University, Beijing 100084, China, and Department of Physics, Beijing Normal University, Beijing 100875, China

ABSTRACT Employing the strong capability of absorbing near-infrared (NIR) light and converting the heat of single-walled carbon nanotubes (SWNTs), and the fast thermal actuation of carbon nanotube−poly(dimethylsiloxane) (PDMS) nanocomposite, in this work we proposed a novel NIR optoelectronic memory (OEM) medium based on a SWNT−PDMS/Ni−PDMS composite bilayer, which was actuated by a low-power-density NIR light illumination. The demo device has shown high performance, including a low operating NIR intensity, a high switching ratio, and a rapid photoresponse with no relaxation. In general, the performance has remarkably outperformed state-of-the-art polymer-based OEM devices. Moreover, the device can be performed reversibly using electric pulses. This study provides a new mechanism to design OEMs and other NIR optic-related devices.

KEYWORDS: optoelectronic memory • near-infrared light • carbon nanotube • polymer • composite

Single-walled carbon nanotubes (SWNT) were previously found to strongly absorb near-infrared (NIR) light, and convert it into heat (1−4). The absorption coefficient is extremely high (10^4−10^5 cm^{-1}), at least 1 order of magnitude greater than that of mercury−cadmium−telluride, the most popular photoconductor for 2D arrays of IR photodetectors (3). The enormous heat emitted can even be utilized to kill cancer cells (2, 4). On the other hand, our previous study revealed that multiwalled carbon nanotube (MWNT) network−poly(dimethylsiloxane) (PDMS) nanocomposites can produce a fast actuation (thermal expansion) when stimulated by an electric signal (5). Combining the above two facts, we consider that SWNT network−PDMS nanocomposites may be thermally actuated by a low-power-density NIR light illumination, thus having application potentials in NIR optic-related devices. In this work, we report a novel NIR optoelectronic memory (OEM) medium based on a SWNT−PDMS/Ni−PDMS composite bilayer. The demo device displays a high performance, including a low operating NIR intensity (on the order of 1 mW/mm^2), a high switching ratio (~10^5), and a rapid photoresponse (<15 ms) with no relaxation. This study provides an alternative approach to the design of high-performance OEM materials and devices, which have great application potentials in optical information storage or other optoelectronic circuits (6, 7), and also provides new ideas to design NIR optic-related devices.

The OEM demo device works by combining the functions of the two composite layers in the medium: the SWNT−PDMS composite layer acts as a NIR light absorber and actuator, and the Ni−PDMS composite layer acts as the conducting channel. The SWNT−PDMS layer absorbs NIR light and thermally expands, driving the underlying Ni−PDMS layer to stretch. Consequently, the conducting network in the Ni−PDMS layer is ruptured; i.e., the device is switched from a low resistance state (LRS) to a high resistance state (HRS). Because of the high NIR absorbance and fast actuation of the SWNT−PDMS composite, the response of the device to NIR light is very sensitive and rapid. After the NIR light is turned off, the conducting network remains ruptured, and thus the device remains in HRS (memorizes). Furthermore, the conducting network can be reconstructed by electric pulses; i.e., the memory device can be performed reversibly. The switching and memory mechanism in the proposed OEM device is totally different from those in previous studies (7−13). In general, the performance has remarkably outperformed state-of-the-art polymer-based OEM devices (7−13). This study may even offer a new application perspective for other photoactuators.

The diameters and lengths of the SWNTs used in this work were around 1−2 nm and 5−30 μm, respectively. The diameters of Ni particles were around 1−3 μm. The intrinsic PDMS rubber is a transparent flexible insulator, with a large coefficient of thermal expansion (~3.1×10^{-4} K^{-1}) (14). The detailed process of fabricating a SWNT−PDMS/Ni−PDMS bilayer is given in the Experimental Section. A high-resolution optical photograph of the cross section of the bilayer is displayed in Figure 1a. The upper layer is the SWNT−PDMS layer and the lower one the Ni−PDMS layer. The individual SWNTs and SWNT bundles are uniformly dispersed in the PDMS matrix (Figure 1b). This is critical, because uniform

* To whom correspondence should be addressed. E-mail: chliu@mail.tsinghua.edu.cn.
Received for review July 26, 2010 and accepted October 1, 2010
[†] Tsinghua University.
[‡] Beijing Normal University.
DOI: 10.1021/am100656x

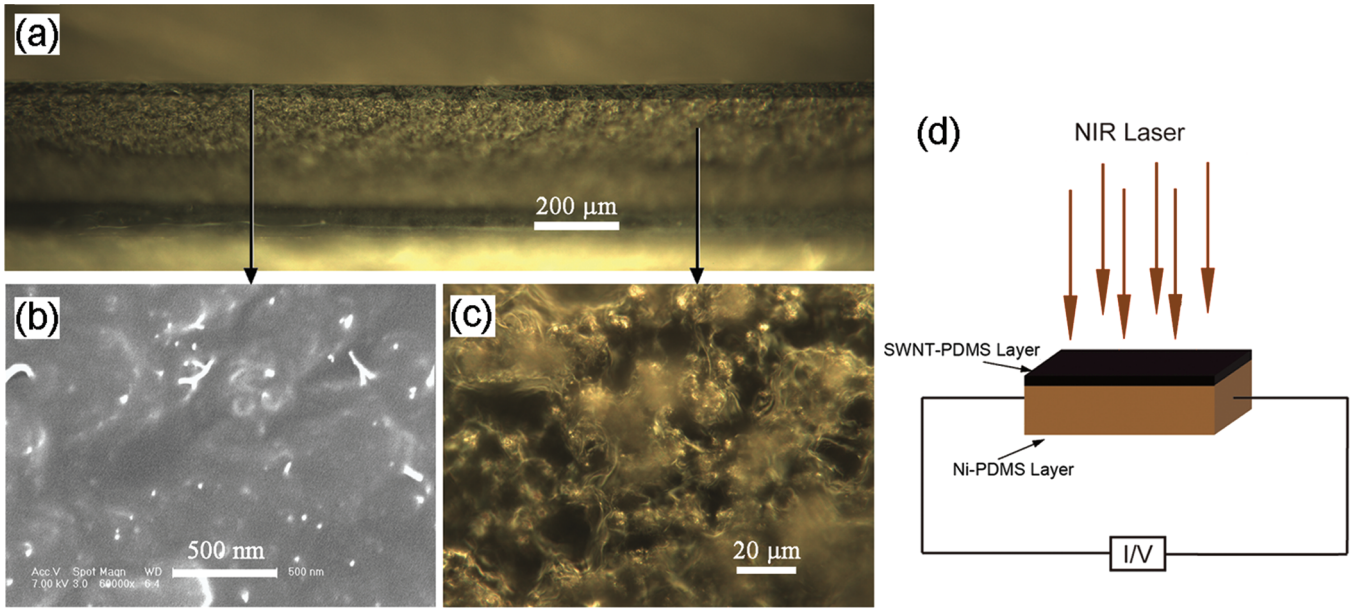

FIGURE 1. (a) Optical photograph of the cross section of the bilayer. (b) Scanning electron microscopy image of the fractured surface of the upper SWNT−PDMS composite layer. (c) Magnified optical photograph of the cross section of the lower Ni−PDMS composite layer. (d) Schematic of the experimental setup for the NIR-induced switching and memory tests.

distribution favors the absorption of NIR light, and also ensures heating of the PDMS matrix at the molecular level (the key factor to fast actuation) (5). From Figure 1c, we can see that Ni particles are also uniformly distributed in the matrix. The bilayer can be easily constructed in a large scale. The SWNT and Ni loadings are 0.59 and 10.26 vol %, respectively. The SWNT loading is slightly below the percolation threshold of the SWNT−PDMS composite (0.7 vol %), which is favorable for the absorption efficiency of NIR light. For Ni−PDMS composites, overloading will lead to a large leakage current in HRS (hence, a lower switching ratio), while underloading will result in a high initialization and RESET voltages. We found that 10.26 vol % is an appropriate content to balance the two factors (the percolation threshold of the Ni−PDMS composite is ~25 vol %). Because both of the loadings are below their own percolation threshold, the OEM medium is insulating at the initial state. The thicknesses of the two layers are 54 and 480 μm, respectively. The thickness of the SWNT−PDMS layer has a strong influence on the thermomechanical behavior. Generally speaking, for too thick layers, because the lower part of the SWNTs in the layer are not exposed to NIR light, the performance of the device hence will be low. On the other hand, for too thin layers, part of NIR light will penetrate the layer and will lower the NIR absorption efficiency. According to our experience, tens of micrometers is an appropriate thickness.

Using the bilayer, we fabricated a series of demo devices (see the Experimental Section), all of which displayed similar NIR OEM behaviors, except for a slight quantitative difference. In this paper, all of the results, unless otherwise specifically indicated, are based on one device of 2.6 × 5.0 mm^2 shape (the separation between the electrodes is 2.6 mm). The bilayer film was placed on a polystyrene substrate. The experimental schematic is illustrated in Figure 1d. The 980 nm NIR laser was provided by a direct diode laser system, and the electrical current/voltage (*I*/*V*) data were obtained with a Keithley 2410 sourcemeter.

Initially, before the NIR light test, a voltage sweep was executed on the device (Figure 2a). This step was to establish the conducting network in the Ni−PDMS layer and bring the device to LRS. Previous studies revealed that conductive filaments are formed in a NiO resistive switch when stimulated by an electric pulse or a voltage sweep (15−17). This is the reason why we choose Ni particles as the conductive fillers. Note that the STOP voltage of the sweep should be larger than 250 V. One may consider that this initializing voltage is very high for practical applications. In fact, for the device here with a length of 2.5 mm, it corresponds to a moderate electric field intensity. For microdevices fabricated using micromachining techniques, we believe that the initializing voltage could be much smaller. After the initial sweep, conducting filaments are formed between adjacent Ni particles, a conducting network was constructed in the Ni−PDMS layer, and the device was set in LRS (see the second sweep). The successful establishment of a conducting network is crucial, paving the way for the OEM device.

Then NIR light tests were carried out (Figure 2b). The power density of the NIR laser was 2.62 mW/mm^2. This value is 6 orders of magnitude smaller than that in the conventional compact disk needed to program (on the order of 10 mW/μm^2) (18). The voltage on the sample was fixed at 0.5 V. From Figure 2b, we can see that when the device was illuminated by the NIR laser, the current immediately dropped (switching from LRS to HRS) in less than 15 ms (time resolution limit of the measurement setup), implying that the conducting network was ruptured. This sudden rupture was attributed mainly to the tension of Ni−PDMS layer driven by actuation of the upper SWNT−PDMS layer. SWNT networks strongly absorb NIR light and heat the PDMS matrix, leading to a fast thermal actuation. While the

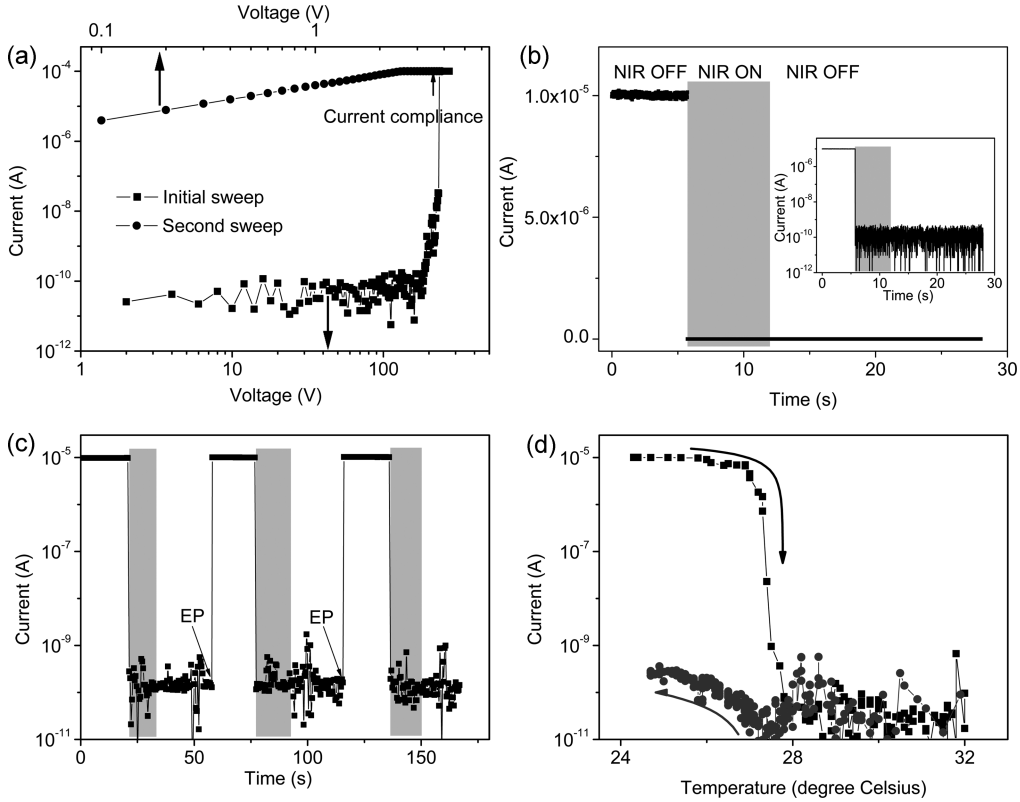

FIGURE 2. (a) Current−voltage plots of the device under two consecutive electric voltage sweeps before NIR tests. The current compliance was set at 1×10^{-4} A. (b) Current versus time response to NIR illumination of the device. The voltage was fixed at 0.5 V. The shaded and unshaded regions mark the NIR-on and -off periods, respectively (hereinafter the same). The inset shows the logarithmic linear plot. (c) Dynamic responses of the device to NIR laser and electric pulses (EPs). EPs with an amplitude of 5 V, and a width of 80 ms were used to switch the device from HRS to LRS. (d) Temperature dependence of the current through the device. The arrows denote the directions of temperature variation.

transportation of heat from the SWNT−PDMS layer to the lower part of the Ni−PDMS layer takes a little time, self thermal expansion of the Ni−PDMS layer probably contributes a secondary part to this process. Of course, self thermal expansion does not hinder the rupture but assists it. An immediate expansive actuation has been observed in random MWNT network−PDMS composites when electric-stimulated (5). Pradhan et al. have also observed a fast and significant NIR photoresponse in the electrical conductivity of SWNT−polycarbonate composites (19). We believe that there is still a large space for improvement of the switching rate of our device by adjusting the NIR laser power density or optimizing the material system. After the laser was turned off, the device remained in HRS (memorized), indicating that the conducting network was still ruptured. The logarithmic linear plot (inset in Figure 2b) reveals that the switching ratio can reach 5 orders of magnitude. These characteristics, such as a low operating laser intensity, a fast response, and a high switching current ratio, indicate that this type of device has tremendous potential in OEMs. According to the coefficient of thermal expansion of PDMS, we estimate that the change in the length of the SWNT−PDMS layer is on the order of 10^{-3} under NIR illumination. Although it is difficult to observe by the naked eye, it is large enough to destroy the conducting filamentary network. In fact, large expansive deformation of a suspended SWNT−PDMS composite film can be easily observed with the naked eye under an appropriate intensity NIR light.

We combine the influences of the NIR laser and electric pulse: the NIR laser switches the device from LRS to HRS, and the electric pulse can recover the device back to LRS. If we define HRS to be the "1" state and LRS the "0" state, and then the effect of the NIR laser is to "write" and that of the electric pulse is to "erase". A small voltage (here 0.5 V) is executed on the device to "read". In one word, this device is operated using optical writing and electrical erasing and reading. The scenario is shown in Figure 2c. The electric pulses were provided by another Keithley 2410 sourcemeter, with an amplitude of 5 V and a width of 80 ms. Note that the amplitude of this RESET electric pulse is not necessarily larger than the voltage needed for the initial establishment of the conducting network (~250 V) because rejoining the filaments is much easier than the initial formation. Voltage sweeping tests revealed that the threshold of the RESET voltage is around 3 V (see the Supporting Information). Figure 2c indicates that the demo device is highly reproducible and the current in LRS is quite stable, which are critical in its practical application as a reversible memory device.

As mentioned above, self thermal expansion of the Ni−PDMS layer can assist the rupture of the conducting network. This is evidenced by the influence of the ambient

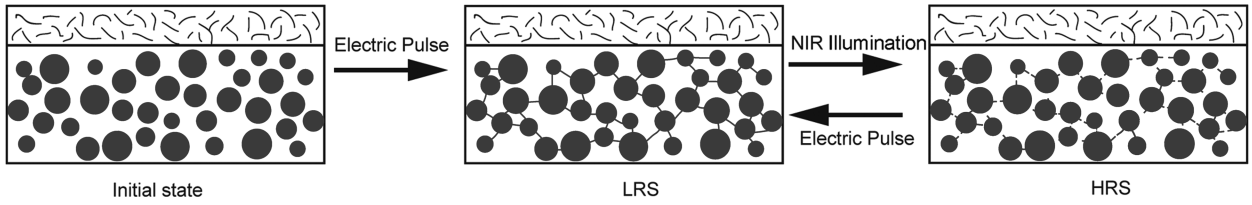

FIGURE 3. Schematic graphics of the structure changes of the device when illuminated by NIR laser and stimulated by electric pulses.

temperature on the device without the use of a NIR laser. The result is displayed in Figure 2d. When it was heated to 27.2 °C, the current abruptly dropped (switched to HRS), indicating that the conductive filament was ruptured. While the device was cooled from 32.0 °C, it remained in HRS, just like the situation in which the NIR laser was turned off (Figure 2b). This interesting temperature-induced switching and memory effect implies that self thermal expansion can also cause rupture of the conducting network. One could notice that the switching temperature (27.2 °C) is very close to room temperature and, hence, may hamper the device in practical applications. In fact, the switching temperature can be adjusted by utilizing different polymer matrixes with different coefficients of thermal expansion. Therefore, we can choose the matrixes with relatively smaller coefficients of thermal expansion to widen the working temperature range.

Here, we briefly discuss the intrinsic conducting mechanism in the Ni−PDMS layer. How the electric pulse affects the conductance in resistive switches varies with different specific systems (20, 21). The proposed models include a filament model, a charge-trap model, an insulator−metal transition, and others. The switching and memory effect in metal−insulator−metal-structured resistive switching memories is generally attributed to the formation and rupture of the filamentary paths (20, 21). Recently, conducting filaments in a NiO resistive switch have been directly observed by Son and Shin using a conducting atomic force microscope (17). The Ni−PDMS composite can be considered as an integration of numerous micro-metal−insulator−metal-structured resistive switches. Our data can also be well interpreted by the filament model. The structure changes in the device induced by an electric pulse and NIR light are schematically illustrated in Figure 3. A large electric pulse (>250 V) initially establishes the conducting network. Tension and thermal expansion of the Ni−PDMS layer ruptures the filaments, while stimulation of the electric pulse rejoins them. This unique property of the Ni−PDMS composite is important for realizing the reversible OEM characteristic in our demo devices. The temperature-induced switching and memory effect (Figure 2d) can be considered as evidence for the filament model because other models, such as the charge-trap and insulator−metal transition models, do not lead to such behavior. Other evidence for the filament model is given in the Supporting Information.

For comparison, devices using a Ni−PDMS single layer without a SWNT−PDMS coating were evaluated (see the Supporting Information). Although they also exhibited NIR OEM characteristics, the switching rates were very low (tens of seconds to minutes) or there was even no switching under NIR laser illumination of similar power densities because of the poor efficiency of NIR absorption of the Ni−PDMS composite. By contrast, because of the electronic transitions between the first or second van Hove singularities (1, 22) and/or the strong electron−phonon interactions (3), the SWNTs efficiently absorb NIR light and convert it into heat. This is the key factor to the excellent performance of the double-layered device. Moreover, two of the unique properties of SWNTs rest with the nanoscaled diameter and the high aspect ratio. The well-dispersed SWNTs behave like numerous nanoheaters that heat the PDMS matrix at the molecular level, resulting in a fast actuation.

Meanwhile, we notice that, during the past few years, studies on organics or polymer-based OEM devices to accompany plastic electronics have progressed (7−13). Those devices are basically fabricated in the field-effect-transistor (FET) geometries and work using a combination of incident light and gate voltage. For instance, Star et al. have fabricated an OEM device by coating a photosensitive polymer onto the channel of a SWNT FET (10). They also found that the spectral response of the device can be adjusted by utilizing different polymers with different absorption characteristics. Chiu et al. have reported an OEM transistor based on a core/shell CdSe@ZnSe quantum dots−poly(3-hexylthiophene) composite, which displayed a high switching ratio of 2700, and maintained it without noticeable decay for 8000 s after the light had been turned off (13). Derycke et al. have demonstrated that, by adjusting the applied gate bias, the photosensitive polymer-coated SWNT FET device can be optimized as an OEM or as an optical switch, in which the switching mechanism involves the trapping of photoexcited electrons at the polymer/dielectric interface (11). This group has reported very recently that two-terminal OEMs based on SWNT FETs (without using the gate electrode) have been achieved, which will simplify the design of integrated OEM devices (7). However, because of the dynamic generation (or recombination) of photoinduced carriers, such types of devices usually need time to reach a stable state with the light ON (or OFF), ranging from seconds to minutes. In this study, we adopted a quite different way for fabricating high-performance OEM devices. The high switching ratio ($\sim 10^5$) and the rapid NIR response (<15 ms) with no relaxation have remarkably outperformed those of the previously reported polymer-based OEM devices. Moreover, there is also no need for a gate electrode in our device, as in Derycke et al.'s (7). In this respect, our work has moved forward on the studies of OEM materials and devices.

On the basis of the working principle of the device, one may argue that, by simply mixing the three components, one-layered OEM materials and devices could also be

achieved. We have constructed a couple of such types of devices, and the test results showed that their switching rates are generally lower than those of the double-layered devices. This is mainly attributed to the unsatisfactory dispersion of the SWNTs in the PDMS matrix. During the fabrication, when Ni powders were added into the SWNT suspension, the tubes intended to adhere to the surfaces of Ni particles and precipitated with them. Therefore, the SWNTs are not able to act as nanoheaters and the performances of the resulting OEM devices are hence low.

Here, we want to state that the OEM materials and devices presented in this work are only prototypes so far. They can further be constructed microscopically and integrated compactly using modern techniques. The thicknesses of both layers and the choice of the matrix can also be adjusted to optimize the performance. The main goal of this paper is to propose an alternative approach to designing OEM device using such a unique structure and mechanism.

To summarize, because of the strong capability of absorbing NIR light and converting heat of SWNTs and the large coefficient of thermal expansion of PDMS rubber, SWNT−PDMS nanocomposites can be easily actuated when being illuminated by a low-power-density NIR light. Employing this unique property of the SWNT−PDMS composite, in this work, we proposed a novel NIR OEM medium based on a SWNT−PDMS/Ni−PDMS composite bilayer. An OEM demo device was constructed, and experimental tests show such a demo device is high performance. Furthermore, the device can be performed reversibly using electric pulses. This work provides a new mechanism to design OEMs and other NIR optic-related devices.

EXPERIMENTAL SECTION

The SWNTs are produced by methane catalytic decomposition over a Co-based catalyst and then experienced deep air oxidation. There is almost no amorphous carbon in this product. The purity of SWNTs is larger than 90 wt %. Their diameters and lengths are around 1−2 nm and 5−30 μm, respectively. Most of the rest of the constituents are carbon nanotubes with small numbers of walls.

Ni powder, DMS, and a tetraethylorthosilicate cross-link reagent (100:94:6 by weight) were first mixed by manual stirring for 10 min and then placed in a vacuum chamber ($\sim 10^3$ Pa) for 5 min to eliminate the air bubbles. The mixture was deposited onto a polystyrene substrate. Then another thin polystyrene plate was laid onto the mixture and pushed until the mixture spread out to be a thin film. This sandwiched structure was put in a baking oven at 50 °C for 24 h. After that, the mixture was solidified (Ni−PDMS composite film), and the upper plate was removed from the film.

The SWNTs were used without further purification. First, they were dispersed in DMS by intensive ultrasonic waves (800 W) for 20 min with the aid of ethyl acetate as a dilute solvent. Then the solvent was evaporated at 80 °C using a baking oven, and the tetraethylorthosilicate cross-link reagent was added into the mixture. The weight ratio of SWNTs, DMS, and the cross-link reagent was 0.75:94:6. After 2 min of manual stirring, the mixture was deposited onto the Ni−PDMS composite film. Then when a cylinder upon the mixture was pushed back and forth a few times, a SWNT−PDMS thin film was formed on the Ni−PDMS film. The mixture was placed in a vacuum chamber ($\sim 10^3$ Pa) for 5 min to eliminate the air bubbles. The SWNT−PDMS composite was solidified in a baking oven at 50 °C for 24 h.

At last, the SWNT−PDMS/Ni−PDMS bilayer was peeled from the underlying polystyrene substrate. The schematic illustration of the fabrication of the bilayer is given in the Supporting Information.

The SWNT−PDMS/Ni−PDMS bilayer was then cut into quadrate shapes to fabricate the devices. Cu wires were employed as electrodes. To enhance the electrical contacts between the bilayer and electrodes, a Ag paint was used. After the solvent in the Ag paint was evaporated, fabrications of the demo devices were finished.

Acknowledgment. This work was supported by the National Basic Research Program of China (Grant 2005CB623606) and the National Natural Science Foundation of China (Grants 50673049 and 10721404).

Supporting Information Available: Schematics of the fabrication of the SWNT−PDMS/Ni−PDMS bilayer, determination of the threshold of the RESET voltage, another evidence for the filament model, and comparison between the performances of the devices based on the bilayer and Ni−PDMS single layer. This material is available free of charge via the Internet at http://pubs.acs.org.

REFERENCES AND NOTES

(1) O'Connell, M. J.; Bachilo, S. M.; Huffman, C. B.; Moore, V. C.; Strano, M. S.; Haroz, E. H.; Rialon, K. L.; Boul, P. J.; Noon, W. H.; Kittrell, C.; Ma, J.; Hauge, R. H.; Weisman, R. B.; Smalley, R. E. *Science* **2002**, *297*, 593–596.
(2) Kam, N. W. S.; O'Connell, M.; Wisdom, J. A.; Dai, H. J. *Proc. Natl. Acad. Sci. U.S.A.* **2005**, *102*, 11600–11605.
(3) Itkis, M. E.; Borondics, F.; Yu, A.; Haddon, R. C. *Science* **2006**, *312*, 413–416.
(4) Chakravarty, P.; Marches, R.; Zimmerman, N. S.; Swafford, A. D. E.; Bajaj, P.; Musselman, I. H.; Pantano, P.; Draper, R. K.; Vitetta, E. S. *Proc. Natl. Acad. Sci. U.S.A.* **2008**, *105*, 8697–8702.
(5) Chen, L. Z.; Liu, C. H.; Hu, C. H.; Fan, S. S. *Appl. Phys. Lett.* **2008**, *92*, 263104.
(6) Liu, C.; Bard, A. J. *Electrochem. Solid-State Lett.* **2001**, *4*, E39-E41.
(7) Agnus, G.; Zhao, W.; Derycke, V.; Filoramo, A.; Lhuillier, Y.; Lenfant, S.; Vuillaume, D.; Gamrat, C.; Bourgoin, J. *Adv. Mater.* **2010**, *22*, 702–706.
(8) Dutta, S.; Narayan, K. S. *Adv. Mater.* **2004**, *16*, 2151–2155.
(9) Podzorov, V.; Pudalov, V. M.; Gershenson, M. E. *Appl. Phys. Lett.* **2004**, *85*, 6039–6041.
(10) Star, A.; Lu, Y.; Bradley, K.; Gruner, G. *Nano Lett.* **2004**, *4*, 1587–1591.
(11) Borghetti, J.; Derycke, V.; Lenfant, S.; Chenevier, P.; Filoramo, A.; Goffman, M.; Vuillaume, D.; Bourgoin, J. *Adv. Mater.* **2006**, *18*, 2535–2540.
(12) Chen, C. C.; Chiu, M. Y.; Sheu, J. T.; Wei, K. H. *Appl. Phys. Lett.* **2008**, *92*, 143105.
(13) Chiu, M. Y.; Chen, C. C.; Sheu, J. T.; Wei, K. H. *Org. Electron.* **2009**, *10*, 769–774.
(14) Govindaraju, A.; Chakraborty, A.; Luo, C. *J. Micromech. Microeng.* **2005**, *15*, 1303–1309.
(15) Gibbons, J. F.; Beadle, W. E. *Solid State Electron.* **1964**, *7*, 785–790.
(16) Kim, D. C.; Seo, S.; Ahn, S. E.; Suh, D. S.; Lee, M. J.; Park, B. H.; Yoo, I. K.; Baek, I. G.; Kim, H. J.; Yim, E. K.; Lee, J. E.; Park, S. O.; Kim, H. S.; Chung, U.; Moon, J. T.; Ryu, B. I. *Appl. Phys. Lett.* **2006**, *88*, 202102.
(17) Son, J. Y.; Shin, Y. H. *Appl. Phys. Lett.* **2008**, *92*, 222106.
(18) Volkert, C. A.; Wuttig, M. *J. Appl. Phys.* **1999**, *86*, 1808–1816.
(19) Pradhan, B.; Setyowati, K.; Liu, H.; Waldeck, D. H.; Chen, J. *Nano Lett.* **2008**, *8*, 1142–1146.
(20) Waser, R.; Aono, M. *Nat. Mater.* **2007**, *6*, 833–840.
(21) Sawa, A. *Mater. Today* **2008**, *11*, 28–36.
(22) Bachilo, S. M.; Strano, M. S.; Kittrell, C.; Hauge, R. H.; Smalley, R. E.; Weisman, R. B. *Science* **2002**, *298*, 2361–2366.

AM100656X